Journal of Sustainable Civil Engineering and Technology
e-ISSN: 2948-4294 | Volume 3 Issue 1 (March 2024), 103-113
https://joscetech.uitm.edu.my
https://doi.org/10.24191/jscet.v3i1.103--113

Evaluation of Post Tension Runway Plate as Retrofitting Simulated with Compression In-Plane Force in Numerical Approach

Muhammad Daffa Fachrur Reza[1*], Sofia W Alisjahbana[1], Muhammad Nuzulul Furqan[1]

[1]Fakultas Teknik dan Ilmu Komputer, Universitas Bakrie, Jakarta, Indonesia

*Corresponding author: 2023669544@student.uitm.edu.my

Received: 19 January 2024/ Accepted: 29 February 2024/ Published online: 29 March 2024

Abstract

The swelling of soil can result from fluctuations in its moisture content, causing it to expand and contract. To mitigate this, structures in direct contact with the soil may require retrofitting. Post-tensioning is one such method that can enhance the stiffness of the structure without altering its properties, thereby helping to prevent damage from expansive soil. This research presents a novel methodology for the design of retrofitting runway pavements using post-tension plates, employing a numerical approach that considers various influencing factors. The methodology integrates the use of differential and Kerr foundation equations, employing the Levy method to ascertain the deflection of the plate structure. Soil parameters are derived from soil sampling and laboratory tests, while loads are determined based on prior research findings and governmental regulations. The findings of the study indicate that the thickness of the plate structure influences its deflection, as greater thickness results in increased stiffness within the structure. Increasing the thickness of the plate enhances stiffness and diminishes deflection. Regarding the direction of post-tensioning, employing tension in both directions proves most effective, resulting in a reduction of deflection by 22.11%. However, this model demands higher costs compared to others due to the increased requirement for tendon post-tensioning. As an alternative, aligning the direction of post-tensioning with the direction of load movement can lead to a reduction of 15.14% in plate deflection, while incurring lower costs compared to applying post-tensioning in both directions.

Keywords: Retrofitting; Post-tension; Numerical approach; Kerr foundation; Runway

1. Introduction

The runway must withstand the dynamic loads generated by aircraft during takeoff and landing operations. Rigid pavements, such as plate structures, are commonly used for runways, with many employing an orthotropic plate structure for their pavement. According to Szilard (2004), these plates possess different flexural rigidities in perpendicular directions, allowing them to withstand two-dimensional forces, bending moments, and transverse shear forces. To improve precision, this study adopts the orthotropic plate type for the runway's plate structure. The possibility of significant amplitude displacement-induced vibrations in runway pavements has been elucidated (Wangsadinata, 2006). These vibrations can result in multi-modal interactions and internal resonance. Therefore, the chosen plate must demonstrate robust stability to ensure optimal performance.

As a pavement, the structure is categorized as a sub-structure that directly interacts with the soil. Expansive soil possesses the capacity to expand or contract in response to fluctuations in soil moisture content. In tropical regions, where heavy rainfall is frequent, constructing pavements in areas with a high risk of expansive soil presents a significant challenge. Expansive soil, also known as clay, is among the most troublesome soil types, as it can cause damage to various civil engineering structures due to its tendency to swell and shrink upon contact with water (Patel, 2019). During periods of heavy rainfall, the soil may expand, consequently elevating

the edge of the plate structure. Conversely, during periods of minimal or no rainfall, the soil may compact, causing the plate structure to either settle with the soil or cantilever over the unaffected soil. Edge lift occurs when the soil expands, whereas center lift happens when the soil dries and compresses (Allred, 2010). As a preventive measure, the retrofitting of structures will be implemented in the study to assess the effectiveness of the chosen retrofitting method, which, in this research, is the post-tensioning method.

The main objective of sustainable construction is to reduce the environmental impact of the construction industry. Implementing various key principles, such as using eco-friendly building materials, increasing energy efficiency, and utilizing green construction technologies, will help achieve this (Wang, 2023). Six fundamental sustainability tenets serve as the foundation for this strategy. These principles focus on the efficient utilization of building materials, which involves minimizing consumption, reusing intact materials, and incorporating recyclable and renewable materials. Additionally, sustainable construction emphasizes the protection of the natural environment and ensures that any new materials used are non-toxic and safe. Ultimately, these endeavors aim to enhance the overall quality of life (Wang, 2023).

Post-tensioning was widely employed for runway construction in Western Europe from 1946 to 1960. When a certain force is applied to a structural member in a way that keeps the internal stresses caused by that force and any other external loads within certain limits, this is called post-tensioning. Post-tensioning a concrete slab entails applying compressive loads before the introduction of service loads or traffic loads. By employing this method, tensile stresses are significantly diminished or even eliminated (Chavez, 2003).

In order to achieve a reasonable level of accuracy, soil-structure interaction is taken into account (Alisjahbana, 2018). In addition to the external loads exerted on the plate, it is essential to calculate the influence of soil-structure interaction to determine plate deflection. Winkler's original soil-structure interaction model has undergone subsequent improvements to increase its accuracy. Findings from evaluations involving the Winkler, Pasternak, and elastic continuum layer foundation models were juxtaposed with those derived from the Kerr foundation model (Kneifati, 1985). Kneifati's conclusion asserts that the Kerr foundation model exhibits superior accuracy in predicting foundation response when compared to the Winkler (Toudehdehghan, 2020) and Pasternak (Khalili, 2018) models. The Kerr foundation model, utilized for the analysis of Kirchhoff-Love's classical plate theory (Ugural, 1981), incorporates intricate equations. Consequently, the Levy method (Sihombing, 2009) is utilized for the computation of plate displacement. This technique encompasses the determination of coefficients in a Fourier series, stabilization of the particular solution for all integer values of m, superimposition of homogeneous and particular solutions, and establishment of boundary conditions for the determined sides of the plate to ascertain constant values such as Am, Bm, Cm, and Dm. The Levy method elucidates the differential equation by incorporating the Kerr Foundation Model equation and establishes boundary conditions for the edges of the plate structure.

Expanding on prior research, this study delves deeper into assessing post-tension plates as retrofitted elements subjected to simulated in-plane compression forces on the Kerr foundation model. The evaluation employs the Levy method and transcendental equations. The research provides multiple advantages for current investigations, contributing to the improvement of planning and designing rigid runway pavements. Considerations include plate thickness, tendon direction, and external loads, such as dynamic loads from aircraft landings. The current planning for the runway plate structure utilizes the ACN-PCN method as outlined by the International Civil Aviation Organization (ICAO) (*Direktorat Jendral Perhubungan Udara*, 2019). This method primarily centers on empirical planning, neglecting factors like vibration effects, deflection, or applied external loads. The objective of this research is to present a novel approach for numerical planning of runway plates, employing differential and Kerr foundation equations in conjunction with the Levy method. The aim is to establish an advanced method for runway plate planning that incorporates comprehensive considerations.

Journal of Sustainable Civil Engineering and Technology
e-ISSN: 2948-4294 | Volume 3 Issue 1 (March 2024), 103-113
https://joscetech.uitm.edu.my
https://doi.org/10.24191/jscet.v3i1.103--113

2. Methods

2.1 Kerr Foundation Soil Modelling

The interaction between soil and structure can be emulated through foundation soil modeling. This modeling approach strives to represent soil-structure interaction by postulating the presence of spring and shear layers in the soil, contingent on its specific soil characteristics. In 1964, Kerr introduced a foundation soil model with the capability to predict a more realistic pressure distribution between the structure and the surface of the foundation soil. This was accomplished by extending the Pasternak foundation soil model and proposing a model comprised of two spring layers, characterized by coefficients k_1 for the upper spring layer and k_2 for the lower spring layer, separated by a soil shear layer with the parameter *Gs*, as depicted in Figure 1.

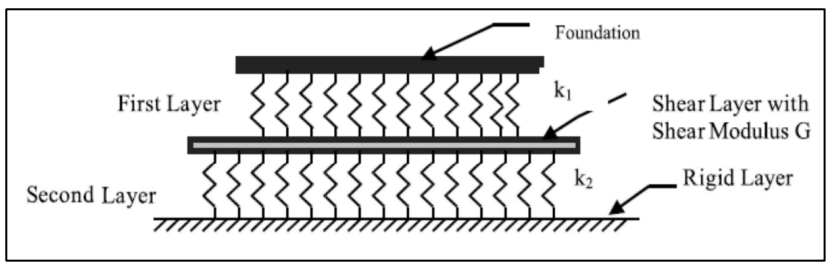

Figure 1. Kerr Foundation Soil Modelling (Kneifati, 1985).

2.2 Levy Method in Plate Differential Equations

The Levy method has proposed scenarios for plate displacement, assuming a plate with a minimum of two fixed points supported at the edges, with boundary conditions tailored to the plate support. This method extends the differential equation using the Kerr Foundation Model equation and defines boundary conditions for the edges of the plate structure. Drawing from this premise, in formulating the differential equation for the plate on the Kerr foundation soil model, the following has been determined:

$$-\left[1+\frac{k_2}{k_1}\right]\left[D_x\frac{\partial^4 w}{\partial x^4}+2B\frac{\partial^4 w}{\partial x^2\partial y^2}+D_y\frac{\partial^4 w}{\partial y^4}+N_x\frac{\partial^2 w}{\partial x^2}+N_y\frac{\partial^2 w}{\partial y^2}+\rho h\frac{\partial^2 w}{\partial t^2}+\gamma h\frac{\partial w}{\partial t}-p(x,y,t)\right]+\frac{Gs}{k_1}\left[D_x\left(\frac{\partial^6 w}{\partial x^6}+\frac{\partial^6 w}{\partial x^4\partial y^2}\right)+2B\left(\frac{\partial^6 w}{\partial x^4\partial y^2}+\frac{\partial^6 w}{\partial x^2\partial y^4}\right)+D_y\left(\frac{\partial^6 w}{\partial y^6}+\frac{\partial^6 w}{\partial x^2\partial y^4}\right)+N_x\left(\frac{\partial^4 w}{\partial x^4}+\frac{\partial^4 w}{\partial x^2\partial y^2}\right)+N_y\left(\frac{\partial^4 w}{\partial y^4}+\frac{\partial^4 w}{\partial x^2\partial y^2}\right)\right]+\frac{Gs}{k_1}\left(\frac{\partial^2}{\partial x^2}+\frac{\partial^2}{\partial y^2}\right)\left(\rho h\frac{\partial^2 w}{\partial t^2}+\gamma h\frac{\partial w}{\partial t}-p(x,y,t)\right)=k_2 w-Gs\left(\frac{\partial^2}{\partial x^2}+\frac{\partial^2}{\partial y^2}\right) \quad (1)$$

Equation (1), as described in reference (Alisjahbana, 2002), delineates the differential equation, which was replaced with the Kerr foundation modeling equation. By employing the Levy method, the boundary condition of the plate structure was established. This equation included external factors such as soil structure interaction, which is represented by k_1, k_2, and *Gs*, which are extracted by soil characteristics; external load, which is expressed by *p(x,y,t)* that gets from the load equation; and in-plane force, which is explained by N_x and N_y and gained by the tendon force to compress the plate, which was obtained by a literature review.

2.3 Plate Stability Analysis

The principles of post-tensioning involve reinforcing the plate structure with tendons embedded during its construction. These tendons are then tensioned after the plate has settled, thereby compressing the edges of the plate and stiffening the structure. In this research, the post-tensioned plate is assumed to experience compression in-plane forces at its edges. The stability of a plate can be demonstrated by its ability to withstand applied in-

plane loads without buckling, within certain magnitudes of these loads. If plane loads exceed the critical buckling loads that the plate can withstand, sudden buckling will occur in the plate structure (Prabowo, 2022). The following equations (2) are presented in nondimensional form to streamline the calculation process:

$$\underline{N}\left[\left[\left(1+\frac{\lambda_2}{\lambda_1}\right)\left(\frac{m^2}{c^2}+n^2\right)\right]+\frac{\mu}{\lambda_1}\left[\frac{m^2}{c^2}+2\frac{m^2n^2}{c^2}+n^4\right]\right]=\lambda_2+\mu\left[\frac{m^2}{c^2}+n^2\right]+\left(1+\frac{\lambda_2}{\lambda_1}\right)\left[\sqrt{\frac{D_x}{D_y}}\frac{m^4}{c^4}+\frac{2B}{\sqrt{D_xD_y}}\frac{m^2n^2}{c^2}+\sqrt{\frac{D_y}{D_x}}n^4\right]+\frac{\mu}{\lambda_1}\left[\sqrt{\frac{D_x}{D_y}}\left(\frac{m^6}{c^6}+\frac{m^4n^2}{c^4}\right)+\frac{2B}{\sqrt{D_xD_y}}\left(\frac{m^4n^2}{c^4}+\frac{m^2n^4}{c^2}\right)+\sqrt{\frac{D_y}{D_x}}\left(\frac{m^2n^4}{c^2}+n^6\right)\right] \quad (2)$$

where *N* is nondimensional critical buckling loads with integer values m and n (m = 1, 2, 3,... and n = 1, 2, 3,...) and using the plate dimension ratio as *c*, which is created by *a/b*. The condition of instability occurs when the plate exhibits a half-wavelength in the x-direction and a half-wavelength in the y-direction, which happens when the integer values m = 1 and n = 1 are reached.

2.4 Natural Frequency

Resonance occurs when the natural frequency equals the frequency of the external load. According to the argument, the natural frequency plays a significant role as an initial check in the performance analysis of plate structures. The natural frequency is determined through a homogeneous solution obtained by simplifying the separation constant. The equation for the natural frequency is described below:

$$(\omega_{mn})^2=-\left[\frac{\beta_{mn}k_1}{\rho h}\right]\left[Gs\left[\frac{m^2\pi^2}{a^2}+\frac{n^2\pi^2}{b^2}\right]+k_1+k_2\right]^{-1} \quad (3)$$

where β_{mn} is the separation constant that is described in the equation below:

$$\beta_{mn}=-\left[1+\frac{k_2}{k_1}\right]\left[D_x\left(\frac{m\pi}{a}\right)^4+2B\left(\frac{m\pi}{a}\right)^2\left(\frac{n\pi}{b}\right)^2+D_y\left(\frac{n\pi}{b}\right)^4-N_x\left(\frac{m\pi}{a}\right)^2+N_y\left(\frac{n\pi}{b}\right)^2\right]-\frac{Gs}{k_1}\left[D_x\left(\frac{m\pi}{a}\right)^6+(2B+D_x)\left(\frac{m\pi}{a}\right)^4\left(\frac{n\pi}{b}\right)^2+(2B+D_y)\left(\frac{m\pi}{a}\right)^2\left(\frac{n\pi}{b}\right)^4+D_y\left(\frac{n\pi}{b}\right)^6-N_x\left(\frac{m\pi}{a}\right)^4-(N_x+N_y)\left(\frac{m\pi}{a}\right)^2\left(\frac{n\pi}{b}\right)^2-N_y\left(\frac{n\pi}{b}\right)^4\right]-k_2-Gs\left[\left(\frac{m\pi}{a}\right)^2+\left(\frac{n\pi}{b}\right)^2\right] \quad (4)$$

Formulating the natural frequency involves removing the damping factor and external factors from equation (1), employing separation constants to simplify equation (3).

2.5 Response of System

2.5.1 Homogeneous Solution

Free vibration occurs when the differential equation removes the damping ratio and external forces, resulting in what is known as a homogeneous solution. This solution comprises two functions: a spatial function representing the x- and y-directions, and a temporal function (time function). After calculating and simplifying both functions, the equation for the homogeneous solution is as follows:

$$w_h=w(x,y,t)=\sum_{m=1}^{\infty}\quad\sum_{n=1}^{\infty}\quad w_{mn}(x,y)T_{mn}(t)$$

$$w_h=w(x,y,t)=\sum_{m=1}^{\infty}\quad\sum_{n=1}^{\infty}\quad[X(x)Y(y)]e^{-\xi\omega_{mn}t}[a_0\,cos(\omega_D)t+b_0\,sin(\omega_D)t] \quad (5)$$

Based on equation (5), *X(x)* and *Y(y)* are spatial functions, and $T_{mn}(t)$ is a temporal function.

Journal of Sustainable Civil Engineering and Technology
e-ISSN: 2948-4294 | Volume 3 Issue 1 (March 2024), 103-113
https://joscetech.uitm.edu.my
https://doi.org/10.24191/jscet.v3i1.103--113

2.5.2 Forced Response

A specific solution to the differential equations involves normalization using the normalization factor Qmn and employs Duhamel integrals to simplify the temporal function, as demonstrated below:

$$T_p(t) = \int_0^t \frac{e^{-\xi\omega mn(t-\tau)}\,\omega_D(t-\tau)}{\rho h\, Q_{mn}\,\omega_D\left[\frac{Gs}{k_1}\left(\frac{m^2\pi^2}{a^2}+\frac{n^2\pi^2}{b^2}\right)-\left(1+\frac{k_2}{k_1}\right)\right]} \int_0^a \int_0^b \left[X^2Y^2\left[\frac{Gs}{k_1}\nabla-\left(1+\frac{k_2}{k_1}\right)\right]p(x,y,\tau)dxdy\right]d\tau \quad (6)$$

$$w_p = w(x,y,t) = \sum_{m=1}^{\infty}\sum_{n=1}^{\infty}[X(x)Y(y)]\int_0^t \frac{e^{-\xi\omega mn(t-\tau)}\,\omega_D(t-\tau)}{\rho h\, Q_{mn}\,\omega_D\left[\frac{Gs}{k_1}\left(\frac{m^2\pi^2}{a^2}+\frac{n^2\pi^2}{b^2}\right)-\left(1+\frac{k_2}{k_1}\right)\right]} \int_0^a \int_0^b \left[X^2Y^2\left[\frac{Gs}{k_1}\nabla-\left(1+\frac{k_2}{k_1}\right)\right]p(x,y,\tau)dxdy\right]d\tau \quad (7)$$

Hence, the force response will be incorporated into the external force function. In the study, the authors utilized formulations for aircraft landing loads, presented as follows:

$$p(x,y,t) = P_0\Omega\, t)\,\delta[x-x(0)]\,\delta[y-y(0)] \quad (8)$$

$$x(0) = v_0.t \quad (9)$$

$$y(0) = \frac{b}{2} \quad (10)$$

A transversal dynamic load is assumed in the constant positions *y = y (0)* and *x = x (0)*. The assumption made pertained to aircraft landing loads, which undergo continuous movement in the y-position at a constant velocity corresponding to the aircraft's landing speed.

2.6 Numerical Parameter

A numerical result is derived for plates of an orthotropic material with thicknesses of 0.10, 0.20, and 0.30 meters. Literature (Wangsadinata, 2006) and governmental regulations (NATO, 2007) served as guides for the selection of plate thickness variation. The foundation parameter was obtained by soil investigation and identification from the industry (CCL, 2017), which was taken by soft soil from Gresik, West Java, as k_1 = 16.26 x 10^5 N/m^2/m, k_2 = 16.26 x 10^6 N/m^2/m, and Gs = 2.86 x 10^5 N/m^2. The data was chosen based on the parameters of potential expansive soil (Patel, 2019; Allred, 2010). Expansive soil is likely to occur in areas with soft soil and clay soil. The soil significantly influences the structure of the plate, expanding and contracting upon contact with water. This can lead to edge lift as the soil expands, while center lift occurs as the soil dries and compresses.

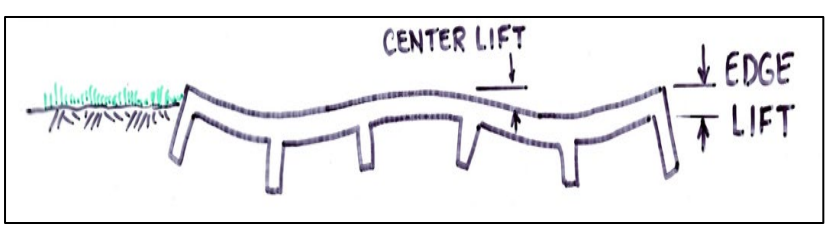

Figure 2. Center Lift and Edge Lift (Allred, 2010)

Journal of Sustainable Civil Engineering and Technology
e-ISSN: 2948-4294 | Volume 3 Issue 1 (March 2024), 103-113
https://joscetech.uitm.edu.my
https://doi.org/10.24191/jscet.v3i1.103--113

The approach of the post-tensioned plate was assumed by the compressed in-plane force uniformly distributed in various directions N_x and N_y; The force was acquired through a literature review of the post-tensioning industry, focusing on technologies such as tendons (CCL, 2017). N_x and N_y were assumed to uniformly distribute force in the x-direction and y-direction of compression force from the tendon. The XM-50 specification, employing 15 strands for the tendon diameter, features a diameter of 15.7 mm with Grade 1860. The maximum force utilized for this research is yet to be specified $N_x = N_y = 3348 \times 10^3$ N. The aircraft landing loads utilized in the research were derived from regulation (NATO, 2007), specifically pertaining to the Boeing 747-400 aircraft equipped with a Rolls-Royce RB211-524H2-T engine, resulting in a load frequency of 1111.1813 radians per second. The widespread commercial use of this aircraft type in Indonesia influenced this decision. The aircraft carried a load of 3.7054×10^6 Newtons with an adjustment vehicle coefficient of 0.7. Additionally, the assumed constant initial landing velocity was 76.891 meters per second.

The plate structure properties employed in the research are outlined in Figure 2. In this context, 'a' denotes the length of the plate, set at 15 meters, while 'b' represents the width of the plate, measured at 7.5 meters. Additionally, the damping ratio is specified as 5%. Previously, the data assumed a rigid pavement for a runway plate structure, constructed with a density of 2400 kilograms per cubic meter.

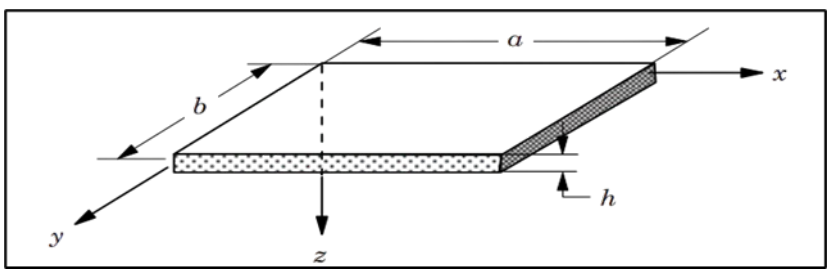

Figure 3. Plate Illustration.

3. Results and Discussion

3.1 Critical In-Plane Force

The critical in-plane force, also known as the buckling force, manifests when the in-plane force, relative to each integer, converges towards the same value. The results shown in Figure 4 show the critical in-plane force for a plate dimension ratio of c = 2 and integer values m = 1 and n = 1.

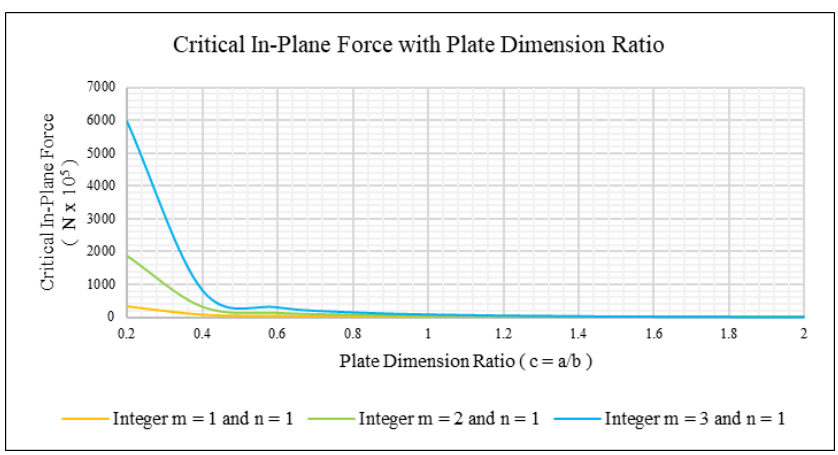

Figure 4. Critical in-plane force

This gives a critical in-plane load value of 3.11 x 105 Newtons. Based on the simulations, the modal integer will get closer to the critical in-plane force at modal integers m = 1 and n = 1. This will cause the dimension plate ratio to go up. Consequently, the research will employ in-plane force compression as a post-tensioning approach below the critical in-plane force value.

3.2 Natural Frequency

The natural frequency serves a crucial role as an initial assessment in the performance analysis of plate structures, as it can anticipate resonance by comparing it with the load frequency. Figure 5 presents the analysis of natural frequency, utilizing 10 modes in each direction. Simulated by *Wolfram Mathematica Software*, the complex equation above was calculated to find natural frequency, which was sampled by the No Post Tension The plate model aims to ascertain the minimum value of natural frequency compared to other models.

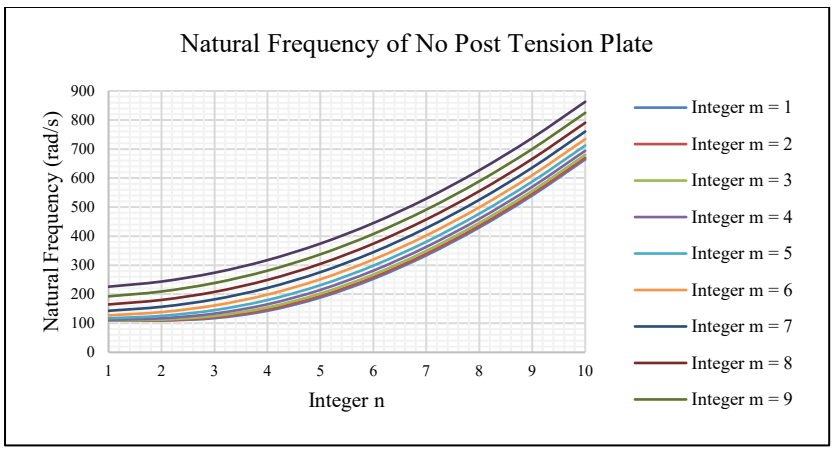

Figure 5. Natural frequency of no post tension plate model

The natural frequency of the plate characterizes the flexural rigidity of the plate structure (Priono, 2020). According to the provided results, the maximum natural frequency value in the model occurred at modal integers m = 10 and n = 10, reaching 862.791 radians per second. It is essential to note that the comparison between the maximum natural frequency value of the system and the load frequency simulated with the aircraft engine frequency should not yield the same value. If they were to coincide, resonance would occur, thereby affecting the performance of the plate structure.

3.3 Post Tension Direction Variation

In order to ascertain the most effective and efficient direction for tendon post-tensioning, the direction of tendon post-tension will be taken into consideration during the analysis. Post-tensioning the tendon will enhance the stiffness of the plate by applying tension to the tendon, resulting in tension reinforcement embedded within the plate structure and compression along the edges of the plate structure. In Figure 6, diverse post-tensioning directions were modeled and calculated to determine the most effective and efficient approach. The analysis of post-tensioning direction will be conducted by examining its influence on the natural frequency of the plate structure.

The conclusion drawn is that the absence of post-tensioning and post-tensioning in the x-direction exhibited similar values, while post-tensioning in the y-direction and overall post-tensioning showed similar values higher than the other two models. Consequently, it is inferred that post-tensioning in the x-direction had a lesser impact on plate stiffness, as indicated by the natural frequency, whereas post-tensioning in the y-direction and overall

Journal of Sustainable Civil Engineering and Technology
e-ISSN: 2948-4294 | Volume 3 Issue 1 (March 2024), 103-113
https://joscetech.uitm.edu.my
https://doi.org/10.24191/jscet.v3i1.103--113

post-tensioning exerted a greater influence on plate stiffness, as reflected by the natural frequency. This could potentially be attributed to the directional movement of the load, which was simulated in the research as the aircraft landing load in the y-direction of the plate.

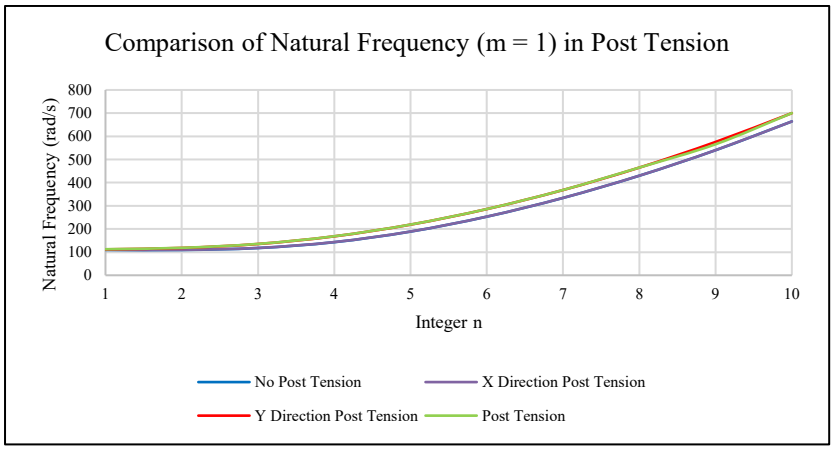

Figure 6. Natural Frequency with Post-Tension Direction Variation

3.4 Plate Performance

3.4.1 Maximum Absolute Deflection

The maximum absolute deflection, compliant with the specifications of the small deflection theory, is determined. In accordance with the theory of small deflections, it is specified that the permissible maximum deflection is 10% of the plate thickness, or 1/10 of the plate thickness modeled in this study (Alisjahbana, 2011).

Table 1. Maximum Absolute Deflection with Post Tension Direction

Post-Tension Direction	Plate Thickness (m)	Maximum Absolute Deflection (m)	Percentage (%)	Commentary
No Post-Tension	0,10	0,001576599	1,577%	Satisfied
	0,20	0,000159705	0,080%	Satisfied
	0,30	4,43921E-05	0,015%	Satisfied
X Direction Post Tension	0,10	0,001393782	1,394%	Satisfied
	0,20	0,000147507	0,074%	Satisfied
	0,30	4,42233E-05	0,015%	Satisfied
Y Direction Post Tension	0,10	0,00133789	1,338%	Satisfied
	0,20	0,000146121	0,073%	Satisfied
	0,30	4,17207E-05	0,014%	Satisfied
Post Tension	0,10	0,001227946	1,228%	Satisfied
	0,20	0,000134273	0,067%	Satisfied
	0,30	4,15575E-05	0,014%	Satisfied

The plate without post-tensioning demonstrates the lowest natural frequency, indicating a relatively higher degree of flexibility. Conversely, post-tensioning the plate serves to decrease the absolute deflection of the plate, thereby enhancing its stiffness. The post-tensioning in both the x and y directions contributed to deflection reduction; nevertheless, the direction of load movement must be taken into account to fully assess the effectiveness of post-tensioning in both directions. Taking into consideration the thickness variations, it can be inferred that a smaller plate thickness leads to increased absolute deflection.

Journal of Sustainable Civil Engineering and Technology
e-ISSN: 2948-4294 | Volume 3 Issue 1 (March 2024), 103-113
https://joscetech.uitm.edu.my
https://doi.org/10.24191/jscet.v3i1.103--113

3.4.2 Time History

Time history, alternatively referred to as a temporal record, is a graphical portrayal that demonstrates the correlation between plate deflection and time. This representation provides a series of deflections corresponding to the modeled time. The maximum absolute deflection occurs when the position of the external loading is at the center of the plate structure, specifically at 0.0975 seconds. This phenomenon arises due to the plate being supported by a simply supported system, resulting in maximum deflection at the mid-span of the structure.

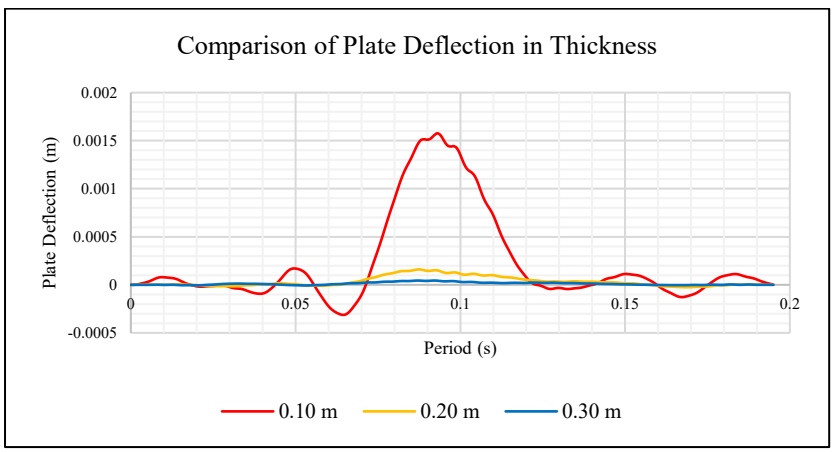

Figure 7. Time history with plate thickness

Based on Figure 7, a comparative analysis of thickness in the no-post tension plate model reveals that a plate thickness of 0.10 m exhibited greater deflection compared to thicknesses of 0.20 m and 0.30 m. The data shown in the figure supports the claim that increased plate thickness results in less deflection. Thickness significantly impacts the stiffness of the plate and affects its flexibility when subjected to external loads. In conclusion, the figure indicates that thicker plates experience reduced deflection.

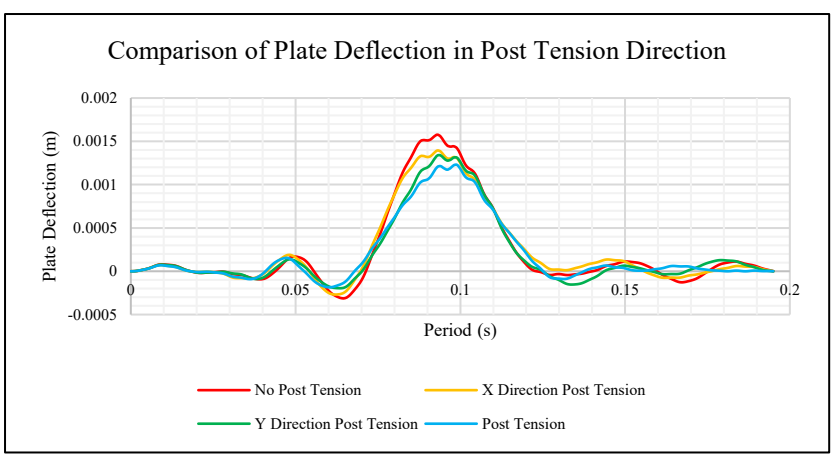

Figure 8. Time History with Post-Tension Direction

In the 0.10 m plate thickness model shown in Figure 8, a comparison of post-tensioning directions shows that the no-post tension direction had the most deflection when compared to the other post-tensioning directions. The post-tensioning, which was modeled with a uniformly distributed compression in-plane force at the edge of the plate, demonstrated effectiveness in reducing the absolute plate deflection. The post-tensioning process

enhanced the stiffness of the plate without altering its properties, such as thickness. The effectiveness of post-tensioning in the x-direction is inferior to that in the y-direction due to the influence of loading movement on the efficacy of the post-tensioning direction. The post-tensioning model, featuring two directions of post-tensioning, proves to be more effective than others due to the dual direction of compression and the elimination of the need to account for loading movement.

4. Conclusion

In the context of runway pavement design, the prevailing approach often relies heavily on empirical methods provided by authoritative bodies. This study seeks to devise a plan for retrofitting runway pavement by taking into account key external factors, such as the orientation of post-tensioned plates, plate thickness, and external dynamic loads—specifically, those associated with aircraft landings. Upon closer examination, it becomes apparent that these factors exert influence on the performance of the plate structure, notably affecting plate deflection.

Concerning the plate thickness, it is observed that thickness influences plate deflection; a thinner plate results in greater deflection, thereby diminishing plate performance. Natural frequency and time history analyses carried out previously show that the determination of plate thickness reveals its impact on plate stiffness. Post-tensioning serves as a retrofitting method aimed at enhancing the stiffness of structures, thereby improving structural performance by reducing the likelihood of excessive deflection. In this study, post-tensioning was modeled using a numerical approach, employing uniformly distributed compression in-plane force along the edge of the plate structure. The most effective orientation for the post-tensioned plate is in both the x and y directions simultaneously, as it reduces plate deflection by 22.11% and obviates the necessity of considering the direction of moving loads. Subsequent to the post-tensioning of the plate in the y direction, aligned with the direction of load movement, a reduction of 15.14% in plate deflection was observed. This phenomenon may be attributed to the alignment of the moving load's direction with the direction of tendon post-tension. When considering cost implications, it should be noted that double-directional post-tensioning requires a greater quantity of tendon, resulting in higher costs. Therefore, for cost efficiency, post-tensioning in the y direction can be adopted, as it necessitates fewer tendons compared to double-directional post-tensioning, thereby resulting in lower overall costs.

The analysis presented in this study offers a comprehensive method for assessing the performance of post-tensioned runway plates under the influence of aircraft landing loads. The general solution for forced response is presented in a manner that allows for its straightforward application to diverse engineering design scenarios. According to the dynamic deflection of the plate, the thickness of the plate and the post-tensioned tendon have a significant impact on the effectiveness and efficiency of plate performance. Their objective is to enhance the stiffness of the plate structure, consequently minimizing the maximum dynamic deflection.

Acknowledgments

The authors would like to express their gratitude to Universiti Teknologi MARA, Shah Alam, Malaysia, for the support and encouragement provided by colleagues, as well as to Universitas Bakrie, Jakarta, Indonesia, for their assistance in providing data support, which greatly contributed to the completion of this paper.

Declaration of Conflicting Interests

All authors declare that they have no conflicts of interest**.**

References

Alisjahbana, S.W. (2002). Dynamic Response of Damped Orthotropic Plates on a Kerr Foundation. *Structural Engineering World Congress, 10,* 370-380.

Alisjahbana, S.W. (2011). *Dinamika Struktur Pelat II*. UB Press.

Alisjahbana, S.W., Alisjahbana, I., Kiryu, S., and Gan, B.S. (2018). Semi Analytical Solution of a Rigid Pavement under a Moving Load on a Kerr Foundation Model. *Journal of Vibroengineering, 20,* 2165-2174.

Allred, B. (2010, January). General Considerations for Post-Tensioned Slabs on Ground. *STRUCTURE Magazine,* 10-12.

CCL (2017) *Post-Tensioning System Civil Engineering Construction*

Chavez, C.I.M., McCullough, B.F., and Fowler, D. W. (2003) *Design of Post-Tensioned Prestressed Concrete Pavement, Construction Guidelines, and Monitoring Plan.* Center for Transportation Research the University of Texas.

Direktorat Jenderal Perhubungan Udara 2019 *Standar Teknis dan Operasional Peraturan Keselamatan Penerbangan Sipil-Bagian 139 (Manual of Standard CASR – Part 139) Volume I Bandar Udara (Aerodrome)* (Jakarta: Kementrian Perhubungan) pp 5-52

Khalili, A., and Vosoughi, A.R. (2018). An Approach for The Pasternak Elastic Foundation Parameters Estimation of Beams using Simulated Frequencies. *Inverse Problems in Science and Engineering, 26,* 1079-1093.

Kneifati, M.C. (1985). Analysis of Plate on a Kerr Foundation Model. *Journal of Engineering Mechanics, 111,* 491-498.

NATO Standarization Agency 2007 *NATO Aircraft Classification Numbers (ACN)/ Pavement Classification Number (PCN)* (Brussels: North Atlantic Treaty Organization) pp 2-54

Patel, A. (2019). *Geotechnical Investigations and Improvement of Ground Conditions.* Woodhead Publishing.

Prabowo, A.R., Ridwan, R., and Muttaqie, T. (2022) On the Resistance to Buckling Loads of Idealized Hull Structure: FE Analysis on Designed-Stiffened Plates. *Design, 8,* 3-46.

Priono, A.B., and Alisjahbana, S.W. (2020). Dynamic Response of Rigid Pavement Plate due to Localized Blast Load. *3rd TICATE 2020, 1007,* 1-7

Sihombing, R.A. (2009). *Analisis Pelat Persegi Panjang dengan Metode Hirzfeld dan Metode M.Levy* B.Eng Thesis, Universitas Sumatra Utara.

Szilard, R. (2004). *Theories of Applications of Plate Analysis.* John Wiley & Sons, Inc.

Toudehdehghan, A. (2020). *Static Analysis of Functionally Graded Coated Plate on Elastic Foundation Based on Levy Method.* The 2nd International Conference on Science and Innovated Engineering, Melaka, Malaysia.

Ugural, A.C., and Fenster, S.K. (1981) *Advance Strength and Applied Elasticity*. Elsevier Science Publishing Co., Inc.

Wang, Y. (2023). *Exploring the Importance of Sustainability in the Construction Industry*. 2023 International Conference on Mechatronics and Smart Systems, Oxford, United Kingdom.

Wangsadinata, W., and Alisjahbana, S.W. (2006). Response Dynamic of Rigid Runway Pavement. *The Tenth East Asia-Pacific Conference on Structural Engineering and Construction, 10,* 375-380.